Hindawi
Mathematical Problems in Engineering
Volume 2019, Article ID 5954104, 16 pages
https://doi.org/10.1155/2019/5954104

Research Article

Structural Damage Identification Based on l_1 Regularization and Bare Bones Particle Swarm Optimization with Double Jump Strategy

Minshui Huang, Yongzhi Lei, and Xifan Li

School of Civil Engineering and Architecture, Wuhan Institute of Technology, Wuhan 430073, China

Correspondence should be addressed to Minshui Huang; huangminshui@tsinghua.org.cn

Received 12 October 2019; Revised 4 December 2019; Accepted 14 December 2019; Published 31 December 2019

Academic Editor: David Bigaud

Structural damage identification (SDI) plays a major role in structural health monitoring (SHM), which has been demanded by researchers to better face the challenges in the aging civil engineering, such as bridge structure and building structure. Many methods have been developed for the application to the real structures, but there are still some difficulties which result in inaccurate, even false damage identification. As a variant of particle swarm optimization (PSO), bare bones particle swarm optimization (BBPSO) is a simple but very powerful optimization tool. However, it is easy to be trapped in the local optimal state like other PSO algorithms, especially in SDI problems. In order to improve its performance in SDI problems, this paper aims to propose a novel optimization algorithm which is named as bare bones particle swarm optimization with double jump (BBPSODJ) for finding a new solution to the SDI problem in SHM field. To begin with, after the introduction of sparse recovery theory, the mathematical model for SDI is established where an objective function based on l_1 regularization is constructed. Secondly, according to the basic theory of the BBPSODJ, a double jump strategy based on the BBPSO is designed to enhance the dynamic of particles, and it is able to make a large change in particle searching scopes, which can improve the search behaviour of BBPSO and prevent the algorithm from being trapped into local minimum state. Thirdly, three optimization test functions and a numerical example are utilized to validate the optimization performance of BBPSO, traditional PSO, and genetic algorithm (GA) comparatively; it is obvious that the proposed BBPSODJ shows great self-adapting property and good performance in the optimization process by introducing the novel double jump strategy. Finally, in the laboratory, an experimental example of steel frame with 4 damage cases is implemented to further assess the damage identification capability of the BBPSODJ with l_1 regularization. From the damage identification results, it can be seen that the proposed BBPSODJ algorithm, which is efficient and robust, has great potential in the field of SHM.

1. Introduction

Structural health monitoring (SHM) has received much attention in recent years due to its importance in transportation service and building structure safety, which offers important economic benefits to human society. As a powerful tool, structural damage identification (SDI) plays a major role in SHM, which is widely used in fields of civil engineering. Generally, the approach of SDI can be divided into two types, one is data-based and the other is model-based. In the group of the data-based method, for instance, artificial neural networks (ANNs) [1–3], support vector machines (SVMs) [4–6], deep learning (DL) [7–9], and related derivative methods are common tricks. However, the application of the aforementioned method is based on the need for providing a large amount of experimental data, but there is a widely recognized obstacle of the data-based approach—feature extraction has been found unstable under inaccurate data conditions [10–13].

The model-based method, such as model updating technology [14], is a conventional way to solve the problem of structural damage identification and location [15]. Even

though this approach is limited by the inaccurate finite element model of the structure, it can obtain accurate damage identification results in location and extent, which have been proved by numerous experiments and research studies [16–18].

Compared to the data-based method, damage identification has been transformed into a mathematical problem solving constrained optimization; therefore, the structural damage identification has become an inverse problem which needs a robust optimization approach to deal with. A key technology named swarm intelligence (SI) optimization algorithms is introduced to overcome the drawbacks of the traditional optimization methods and considered to handle complex structural damage identification problems. For instance, artificial bee colony (ABC) algorithm [19], particle swarm optimization (PSO) [20], firefly algorithm (FA) [21], and artificial fish swarm algorithm (AFSA) [22].

As for the traditional PSO algorithm, there are some researchers who are trying to improve and overcome its drawbacks. Hu [23] designed a mutation operator similar to PSO iteration to provide individuals a direction in the evolutionary process, which can produce potential good individuals. He et al. [24] proposed a neighbourhood-based mutation operator strategy which is introduced into PSO to achieve the purpose of enhancing population diversity.

In this study, a novel SI method named bare bones particle swarm optimization with double jump (BBPSODJ) is originally applied to SDI. Bare bones particle swarm optimization (BBPSO) was proposed by Kennedy and Eberhart in 2003 [25], which is famous for its merits, such as parameter-free and easy applying [26]. Compared to the traditional PSO, BBPSO provides a new approach to solve multimodal optimization problems. However, its basic forms are of little value, and it is short of efficiency and robustness. Hence, some studies concentrate on modifying basic BBPSO. To enhance the global search ability of BBPSO, Guo and Sato proposed a dynamic reconstruction strategy that can select some elite particles to reconstruct the particle swarm [27]. Then, fission and fusion can work together for searching the global optimal value. [28].

On the other hand, there are some researchers who focused on keeping swarm diversity and proposed some measures to enhance the diversity of the swarm, such as separate iteration [26] and dynamic local search strategies [29]. Liu et al. [30] utilized a novel disruption strategy, originating from astrophysics, to shift the abilities between exploration and exploitation during the search process, and an opposition-based learning (OBL) modified strategy was further investigated [31].

There remains a need for an efficient method that can solve the problem of premature convergence. Krohling and Mendel considered to introduce a jump strategy to BBPSO when no fitness improvement is observed [32], and some simulations show that large-scale global optimization can be solved by BBPSO with Gaussian jump [33]. Qiu attempted to help the stagnated particles make a large change in their searching trajectory by designing an adaptive chaotic jump strategy [34]. Meanwhile, distribution-guided jump operation [35] and componentwise jumping mechanism [36] can also make good effect.

In addition, in most SDI problems, the damage of the structure is always sparse; it means that there are only several damaged elements. The vector of damage is a sparse vector, and the equation is underdetermined which cannot obtain a unique solution. Some researchers have recently introduced a technique named sparse recovery to handle the problems mentioned above. Zhou et al. [37] used the first few frequency data of a cantilever beam to verify the sparse damage situation, and the antinoise effect was reflected. Then, the mode shape was introduced to enhance the accuracy of damage location [38]; at the same time, the method of selecting a regularization parameter was proposed [39]. It seems that the sparse recovery theory has a good effect on damage detection. Furthermore, some comparative studies on damage identification with Tikhonov regularization and sparse regularization were stated by Zhang and Xu [40], and the sparse regularization approach was confirmed to be better than Tikhonov regularization.

To overcome the drawback of basic BBPSO, such as local optimal, slow convergence, and lower computing efficiency, a novel optimization algorithm, which is named bare bones particle swarm optimization with double jump (BBPSODJ), is first proposed here; a double jump strategy is incorporated to solve the problem of local optima state in the process of iteration and keep the diversity of particles. Firstly, an objective function based on l_1 regularization is constructed with BBPSODJ to detect damage. Three optimization test functions are provided to analyse the optimization performance of BBPSODJ, BBPSO, and PSO. Secondly, the damage identification problem of a numerical example is solved by BBPSODJ. The outcomes illustrate that the proposed algorithm is better at computational accuracy and convergence efficiency than basic BBPSO, traditional PSO, and genetic algorithm (GA). BBPSODJ combined with l_1 regularization objective function has good noise robustness; it is more suitable for damage identification problems. Finally, the method proposed is adopted to identify the damage of an experimental example of 3-story steel frame structure, whose performances show that BBPSODJ can not only determine the location of damage but also quantify the severity.

2. Sparse Damage Identification Model

2.1. Sparse Recovery Theory. Recently, the sparse recovery theory is proposed to recover an original signal from a polluted signal. In sparse recovery theory, a signal is considered as a linear system of equations:

$$\mathbf{y}_{m\times 1} = \mathbf{A}_{m\times n}\mathbf{x}_{n\times 1}, \tag{1}$$

where $\mathbf{y}_{m\times 1}$ is the measurement signal with the length of m; $\mathbf{x}_{n\times 1}$ is a sparse vector with the length of n; and $\mathbf{A}_{m\times n}$ is a sensing matrix of size $m \times n$.

There are infinite solutions since the equation is underdetermined ($m < n$), however, the sparsest one is mostly desired. The solution of equation (1), which is convex

and much easier to handle, can be obtained by solving the optimization as follows:

$$\begin{aligned} &\min \quad \|\mathbf{x}\|_1 \\ &\text{s.t.} \quad \mathbf{y} = \mathbf{A}\mathbf{x}, \end{aligned} \tag{2}$$

where $\|\mathbf{x}\|_1$ is the l_1-norm of the sparse vector x. In fact, the signal is always corrupted with environmental noise; in that situation, equation (2) can be written as

$$\begin{aligned} &\min \quad \|\mathbf{x}\|_1 \\ &\text{s.t.} \quad \|\mathbf{A}\mathbf{x} - \mathbf{y}\|_2 \le \varepsilon, \end{aligned} \tag{3}$$

where ε denotes environmental noise.

2.2. Description of Structural Damage. The damage of structures can be quantified through a scalar variable θ, whose values are between 0 for the undamaged element of structure and 1 for a damaged element. The damage can be described by a decrease in the stiffness of the element:

$$k_i^d = (1 - \theta_i) k_i^u, \tag{4}$$

where k_i^d and k_i^u are the damaged and undamaged local stiffness matrices of the i-th element in the finite element method, respectively, and θ_i is the i-th element stiffness reduction factor (SRF).

In the finite element method, the global stiffness matrix of a structure is acquired by the transformation and assemblage of the element stiffness matrices. The damaged local stiffness matrix k_i^d is transformed into K_i^d, which is the damaged element stiffness matrix in the global coordinate system by the use of the transformation matrix T:

$$K_i^d = T^T k_i^d T. \tag{5}$$

The damaged element stiffness matrix in the global coordinate system K_i^d is then expanded into $(N \times N)$ matrix denoted by $\overline{K}_i^d$, where N is the number of degrees of freedom (DOFs) of the structure. The damaged global stiffness matrix K_d is acquired by summation of $\overline{K}_i^d$ for all elements:

$$K_d = \sum_{e=1}^{\text{nele}} \overline{K}_i^d, \tag{6}$$

where nele is the total number of elements in the structure.

2.3. l_1 Regularization Objective Function. In structural health monitoring (SHM), structural dynamic characteristics, such as natural frequencies and mode shapes, are widely utilized to detect structural damage. But, the structural dynamic characteristics obtained by experimental vibration test are always polluted by environmental noise. Moreover, the damage vector is a sparse vector, so the sparse recovery theory can be introduced to damage identification.

According to equation (3), the structural damage vector can be obtained by solving the equation as follows:

$$\begin{aligned} &\min \quad \|\boldsymbol{\theta}\|_1 \\ &\text{s.t.} \quad \|\mathbf{S}\boldsymbol{\theta} - \Delta\boldsymbol{\lambda}\|_2 \le \varepsilon, \end{aligned} \tag{7}$$

where $\mathbf{S}$ is a sensitivity matrix of dynamic characteristics with respect to element stiffness reduction factor, which can be calculated by differential or partial differential method and $\Delta\boldsymbol{\lambda} = \boldsymbol{\lambda}^e - \boldsymbol{\lambda}^a$ in which $\boldsymbol{\lambda}^e$ and $\boldsymbol{\lambda}^a$ are experimental and analytical dynamic eigenvalues, respectively.

Equation (7) can be further written as [37]

$$\begin{aligned} &\min \quad \|\boldsymbol{\theta}\|_1 \\ &\text{s.t.} \quad \|\lambda(\boldsymbol{\theta}) - \boldsymbol{\lambda}^e\|_2 \le \varepsilon, \end{aligned} \tag{8}$$

where $\boldsymbol{\lambda}(\boldsymbol{\theta}) = \mathbf{S}\boldsymbol{\theta} + \boldsymbol{\lambda}^a$. Thus, the damage identification problem is transformed to solving a l_1-norm minimum $\boldsymbol{\theta}$ problem, and its goal is to find the best solution that narrows the discrepancy between experimental and analytical dynamic characteristics. Therefore, equation (8) is equivalent to the following l_1 regularization problem [37]:

$$\text{obj} = \left\|\boldsymbol{\lambda}(\boldsymbol{\theta}) - \boldsymbol{\lambda}^e\right\|_2^2 + \beta\|\boldsymbol{\theta}\|_1, \tag{9}$$

where $\beta > 0$ is the regularization coefficient, which can be obtained by the L-curve approach [41].

As for specific damage identification problem, the natural frequencies and mode shapes are adopted, and according to equation (9), the l_1 regularization objective function for damage identification is obtained [38]:

$$\text{obj} = \frac{1}{m}\sum_{i=1}^{m}\left[\frac{f_i^a(\boldsymbol{\theta}) - f_i^e}{f_i^e}\right]^2 + \frac{1}{m \times np}\sum_{i=1}^{m}\sum_{j=1}^{np}\left[\phi_{ij}^a(\boldsymbol{\theta}) - \phi_{ij}^e\right]^2 + \frac{\beta}{n}\|\boldsymbol{\theta}\|_1, \tag{10}$$

where f_i^a and f_i^e are the i-th analytical and experimental natural frequencies, respectively; ϕ_{ij}^a and ϕ_{ij}^e are the i-th analytical and experimental mode shapes at j-th point; m is the number of modes; and np is the number of measurement points. Meanwhile, the mode shape is processed by modal scaling factor as defined as follows [38, 42]:

$$\begin{aligned} \text{MSF}\left(\widetilde{\phi}_i^a, \phi_i^e\right) &= \frac{\left(\widetilde{\phi}_i^a\right)^T\left(\phi_i^e\right)}{\left(\widetilde{\phi}_i^a\right)^T\left(\widetilde{\phi}_i^a\right)}, \\ \phi_i^a &= \widetilde{\phi}_i^a \times \text{MSF}, \end{aligned} \tag{11}$$

where $\widetilde{\phi}_i^a$ is the i-th analytical mode shape before adjustment.

3. Bare Bones Particle Swarm Optimization with Double Jump

3.1. PSO and BBPSO. Particle swarm optimization (PSO), which was developed by Eberhart and Kennedy in 1995 [43], is a group intelligent optimization algorithm. It gives a simple and efficient route to solve the optimization problem, especially for structural damage identification.

In the standard PSO algorithm, there are some particles that are generated randomly in the D-dimensional search space. Position and velocity, which are properties of the particle, will change when the particle approaches the global optimal value. Mathematically, the velocity V of the i-th particle is updated according to the following formula:

$$V_i^{t=t+1} = \omega V_i^t + c_1\alpha_1 \cdot \left(gbest - P_i^{t=t+1}\right) + c_2\alpha_2 \cdot \left(pbest - P_i^{t=t+1}\right), \tag{12}$$

where i is the i-th particle; t is the number of current iteration; $c_1 = c_2 = 2$ are the learning factors [44]; α_1 and α_2 are random constants in the range of [0, 1], respectively; and *gbest* and *pbest* are global optimal particle and local best position, respectively. The inertia weight ω can be calculated as [45]

$$\omega = \omega_{\max} - \frac{t \cdot \left(\omega_{\max} - \omega_{\min}\right)}{N_{\text{iteration}}}, \tag{13}$$

where $\omega_{\max}$ and $\omega_{\min}$ denote the maximum and minimum inertia weight, respectively, and $N_{\text{iteration}}$ is cumulative iteration number. And the iteration flowchart of PSO is shown in Figure 1.

The position P of the i-th particle is

$$P_i^{t=t+1} = P_i^t + V_i^{t=t+1}. \tag{14}$$

Compared to the traditional PSO, BBPSO provides a new approach to solve the optimization problems. In the BBPSO, the velocity updating formula is replaced. Meanwhile, a different updating mechanism is raised, which uses a Gaussian distribution with the information of the best local and global positions to update the particle's position. The updated formula for particle's position in the BBPSO is given as [25]

$$P_i^{t=t+1} = N(\mu, \sigma), \tag{15}$$

where $N(\mu, \sigma)$ is a Gaussian random number with mean value, $\mu = (pbest + gbest/2)$, and $\sigma = |gbest - pbest|$. And the flowchart of BBPSO and PSO is shown in Figure 1.

3.2. Improved BBPSO Algorithm with Double Jump Strategy. Despite some endeavours in the improvement of PSO, unfortunately, BBPSO still converges around local optima when optimizing functions with many local optima in high dimensional search space, and there remain numerous challenges that limit its practical application. To obtain a global optimal solution accurately with fast convergence speed, a novel strategy named double jump strategy is implemented to improve basic BBPSO. The main idea of double jump strategy could be summarized up as follows:

(1) To assess the variation of fitness, if the fitness of the current iteration has improved compared to the former iteration, the particle's position is updated by equation (15).

(2) By monitoring the fitness, if there is no fitness improvement with the number of iterations, it means stagnation. Then, a parameter, named as stagnation number (SN), is defined to record the number of each particle in a stagnation state. When SN achieves a prespecified maximum stagnation number, the related particle is considered to jump to a new point [32].

(3) The current best particle is defined as a reference point, the Euclidean distance between the reference point and others is calculated in turn, and the average value of the distance is obtained.

(4) For a particle of current iteration which is considered to jump, if the Euclidean distance between it and the reference point is smaller than the average distance, the particle's position is updated as follows:

$$P_i^{t=t+1} = pbest \cdot \left(1 + \eta_1 \cdot N(0,1)\right). \tag{16}$$

On the contrary, if the distance is bigger than the average distance, the updating equation is

$$P_i^{t=t+1} = pbest \cdot \left(1 + \eta_2 \cdot N(0,1)\right), \tag{17}$$

where η_1 and η_2 are the jumping scaling factors; generally speaking, $\eta_1 < \eta_2$; $N(0,1)$ is a random number generated according to a Gaussian distribution.

The flowchart of BBPSODJ is shown in Figure 2. Meanwhile, the pseudocode is given to explain the developed algorithm, which is shown as follows (Algorithm 1):

The introduction of double jump strategy can not only enhance the ability of BBPSO to escape local optimum but also reduce the blindness of jumping operation, so the global optimum and fast convergence speed can be ensured.

3.3. Performance Evaluation of the Proposed Algorithms. In this section, to compare the computing performance of BBPSODJ, three common algorithms, such as BBPSO, PSO, and genetic algorithm (GA) [17], are introduced. Three test functions, Ackley, Schwefel, and Schaffer (Figure 3), are utilized to test the algorithms. The parameters of the four algorithms are listed in Table 1. After running the algorithms with 200 times iterations for 7 loops, the best and average solutions are shown as in Table 1. And the iterative curves of the algorithms are shown in Figure 4.

(1) Ackley:

$$\begin{aligned} f_{\text{Ackley}}(x) = {} & -20\exp\left(-0.2\sqrt{\frac{1}{10}\sum_{i=1}^{10} x_i^2}\right) \\ & - \exp\left(\frac{1}{10}\sum_{i=1}^{10}\cos\left(2\pi x_i\right)\right) \\ & + 20 + \exp(1), \quad |x_i| \le 32.768. \end{aligned} \tag{18}$$

(2) Schwefel:

$$f_{\text{Schwefel}}(x) = 837.9658 - \sum_{i=1}^{2} x_i \sin\left(\sqrt{|x_i|}\right), \quad -500 \le x_i \le 500. \tag{19}$$

(3) Schaffer:

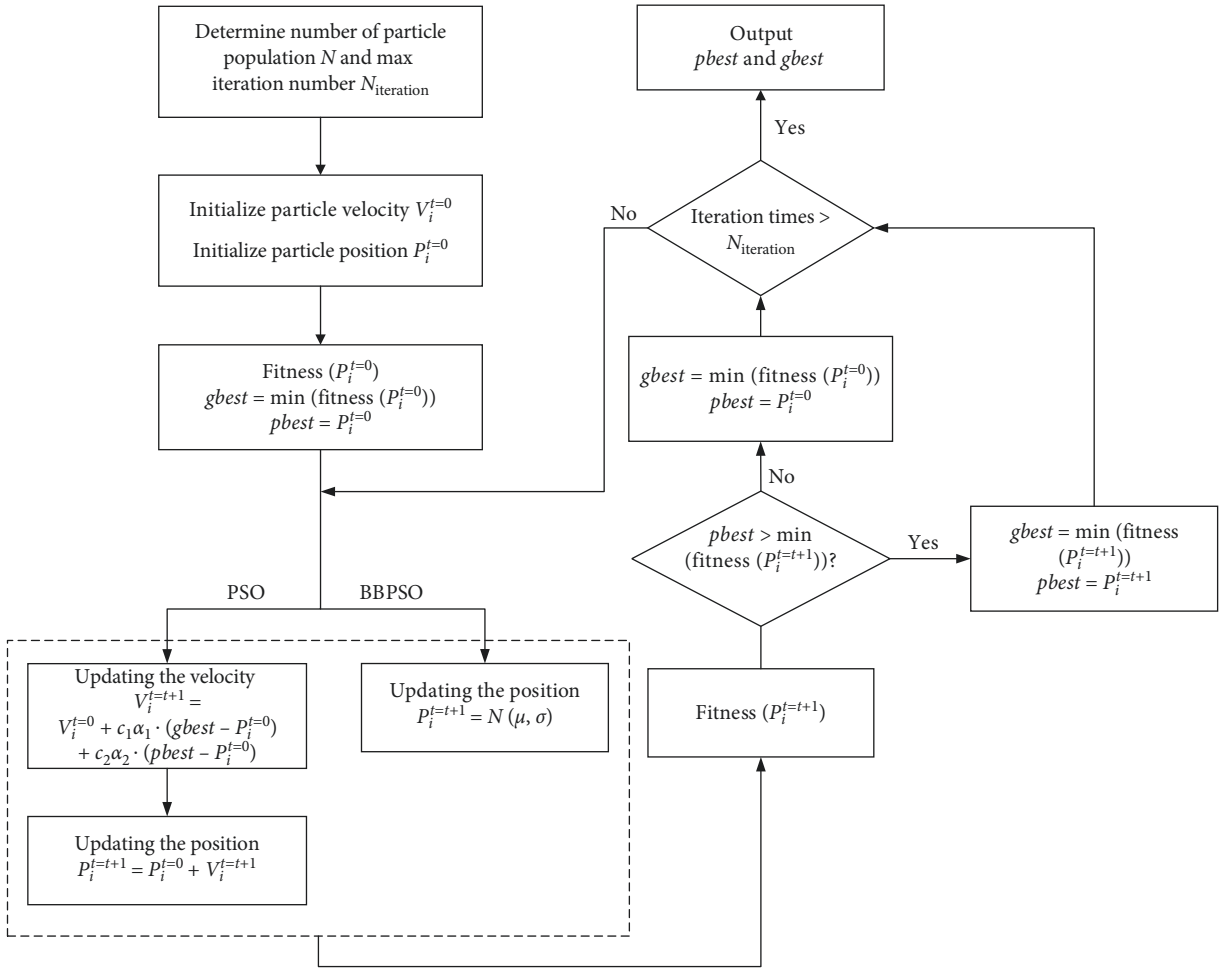

Figure 1: Flowchart of BBPSO and PSO.

$$f_{\text{Schaffer}}(x) = 0.5 + \frac{\left(\sin\sqrt{x_i^2 + x_{i+1}^2}\right) - 0.5}{\left[1 + 0.001\left(x_i^2 + x_{i+1}^2\right)\right]^2},$$
$$-10.0 \le x_i \le 10.0. \tag{20}$$

From Table 1 and Figure 4, it can be seen obviously that the performance of BBPSODJ is better than GA, PSO, and basic BBPSO at convergence speed and computational efficiency. The reason may be that double jump strategy is used to solve the converging problem. And BBPSODJ, the improved version of BBPSO, shows great self-adapting property in the optimization process and good performance by introducing the novel strategy.

4. Damage Identification Using Numerical Example

A 31-bar truss structure shown in Figure 5, which is developed by MATLAB, is utilized to test the damage identification effects of the three algorithms. The lengths of the exterior and interior bar are 1 m and 1.41 m, respectively, and the cross-sectional area is 0.004 m^2, Young's modulus is $E = 200$ GPa, and the mass density is 7800 kg/m^3. The total numbers of elements and nodes are 31 and 14, respectively.

Three damage cases without environmental noise, single-bar damage, two-bar damage, and multibar damage, are introduced. Meanwhile, based on the previous three cases, 5% random noise is considered to simulate the actual measurement and to test the antinoise capability of the algorithms.

The six damage cases are shown as follows:

(1) Case 1: stiffness loss by 15% in element #12

(2) Case 2: stiffness loss by 10% in element #5 and 15% in element #12

(3) Case 3: stiffness loss by 10% in element #5, 15% in element #12, and 20% in element #25

(4) Case 4: stiffness loss by 10% in element #5 (5% random noise)

(5) Case 5: stiffness loss by 10% in element #5 and 15% in element #12 (5% random noise)

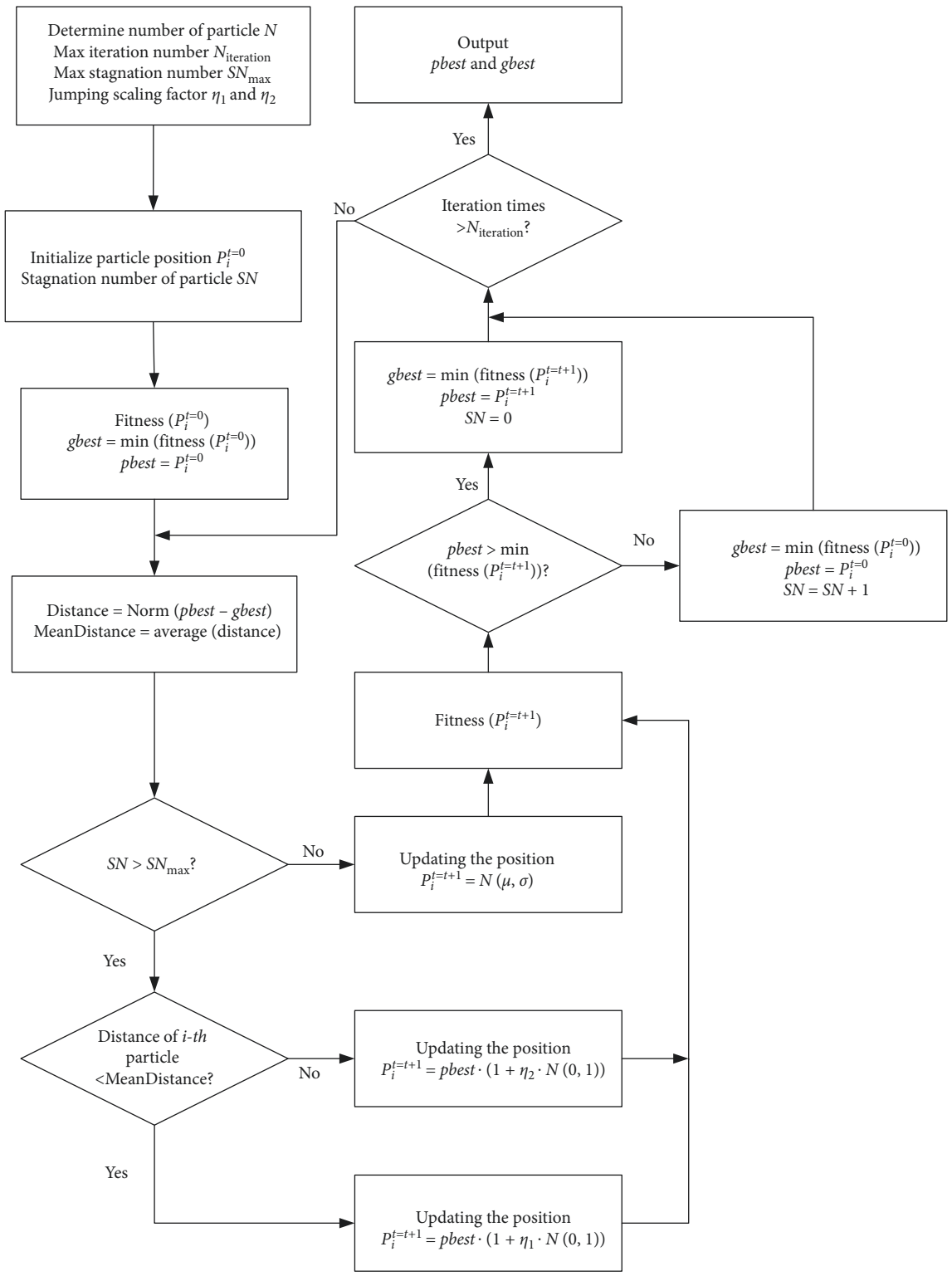

Figure 2: Flowchart of BBPSODJ.

(6) Case 6: stiffness loss by 10% in element #5, 15% in element #12, and 20% in element #25 (5% random noise)

The random noise can be simulated by the equations shown as follows [46]:

$$\phi_j^k = \phi_j (1 + \eta \, \text{rand}), \tag{21}$$

where ϕ_j and ϕ_j^k are the j-th mode shape without noise and polluted with noise; η is the noise level; and rand is a random number in the range of [–1, 1].

Input parameters: number of Particles P, the jumping scaling factors η_1 and η_2, the maximum stagnation number $SN_{\max}$, and the dimension of the objective function d.
// random generation of a population of particles with position x_i using uniform probability // distribution, where $\overline{x}$ and $\underline{x}$ are the lower and upper bound respectively,
// And the initial stagnation number for each particle $SN_i = 0$
FOR each particle i
  $x_i = x + (\overline{x} - \underline{x}) \cdot U(0, 1)$
  $pbest_i = x_i$
  $SN_i = 0$
END FOR
$gbest = \arg\min_{i=1}^{P}\{f(x_i)\}$ // global best particle
DO
  FOR each particle i
    $\text{Dist}_i = \text{Norm}(pbest_i - gbest)$
    $\text{MeanDist} = \text{average}(\sum_{i=1}^{P} \text{Dist})$
  IF $SN_i > SN_{\max}$
  IF $\text{Dist}_i < \text{MeanDist}$ THEN
    Update the position x_i according to (16) // jump with small scaling factor
  ELSE
    Update the position x_i according to (17) // jump with large scaling factor
    END IF
  ELSE
    Update the position x_i according to (15)
  END IF
  IF $f(x_i) < f(pbest_i)$ THEN // update local best
    $pbest_i = x_i$
    $SN = 0$ // reset after a jump
  ELSE
    $SN = SN + 1$ // no improvement in fitness
  END IF
  IF $f(x_i) < f(gbest_i)$ THEN // update the global best
    $gbest = pbest_i$
  FOR each variable j of particle i // limit position
    IF $x_{i,j} > \overline{x}$ THEN $x_{i,j} = pbest_{i,j}$
    IF $x_{i,j} < \underline{x}$ THEN $x_{i,j} = pbest_{i,j}$
  END FOR
WHILE termination condition not met
Output: $gbest$

Algorithm 1

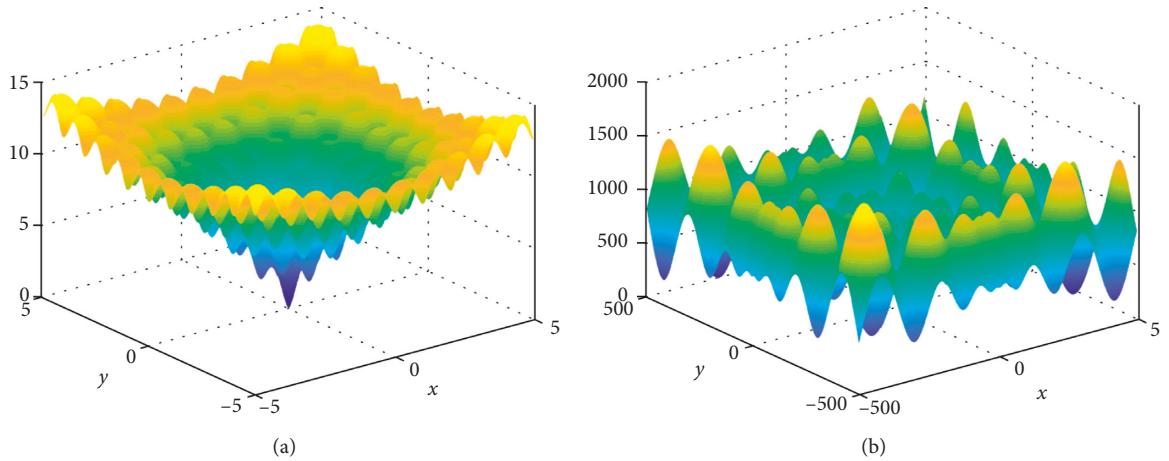

Figure 3: Continued.

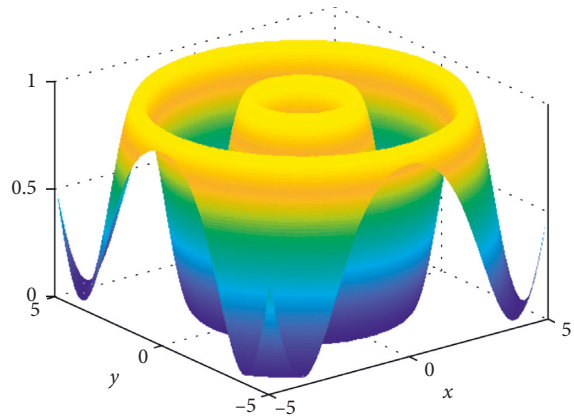

(c)

Figure 3: Single-objective functions: (a) Ackley; (b) Schwefel; (c) Schaffer.

Table 1: Optimal result of three single-objective functions.

Test function	Algorithms	Parameters	Best optimal value	Average optimal value
Ackley	PSO	$c_1 = c_2 = 2$ [44], $\omega_{\min} = 0.4$, $\omega_{\max} = 0.9$ [45] Number of particles = 100	1.479929$e-05$	1.453575$e-04$
	BBPSO	Number of particles = 100	1.23836$e-09$	3.824170$e-06$
	BBPSODJ	$SN_{\max} = 5$, $\eta_1 = 0.01$, $\eta_2 = 0.05$ Number of particles = 100	4.590044$e-10$	2.195117$e-09$
	GA	$Pc_{\max} = 0.8$, $Pc_{\min} = 0.6$ $Pm_{\max} = 0.05$, $Pm_{\min} = 0.001$ Number of population = 100	0.0011292069	0.4989836612
Schwefel	PSO	$c_1 = c_2 = 2$ [44], $\omega_{\min} = 0.4$, $\omega_{\max} = 0.9$ [45] Number of particles = 100	2.5455132$e-05$	2.5455132$e-05$
	BBPSO	Number of particles = 100	2.5455132$e-05$	2.5455132$e-05$
	BBPSODJ	$SN_{\max} = 5$, $\eta_1 = 0.01$, $\eta_2 = 0.05$ Number of particles = 100	2.5455132$e-05$	2.5455132e-05
	GA	$Pc_{\max} = 0.8$, $Pc_{\min} = 0.6$ $Pm_{\max} = 0.05$, $Pm_{\min} = 0.001$ Number of population = 100	2.5455132$e-05$	0.0147555699
Schaffer	PSO	$c_1 = c_2 = 2$ [44], $\omega_{\min} = 0.4$, $\omega_{\max} = 0.9$ [45] Number of particles = 100	0	2.899789$e-03$
	BBPSO	Number of particles = 100	0	6.939936$e-03$
	BBPSODJ	$SN_{\max} = 5$, $\eta_1 = 0.01$, $\eta_2 = 0.05$ Number of particles = 100	0	8.243193$e-05$
	GA	$Pc_{\max} = 0.8$, $Pc_{\min} = 0.6$ $Pm_{\max} = 0.05$, $Pm_{\min} = 0.001$ Number of population = 100	0.00245585817	0.00245585817

Note. *Pc* and *Pm* are the probabilities of crossover and mutation, respectively.

To evaluate the capability of damage identification, the parameters of three algorithms are the same as Section 3.3. The identification results are shown in Figure 6.

As shown in Figures 6(a)~6(f), for a series of the particle swarm algorithms, such as PSO, BBPSO, and BBPSODJ, the identification results of PSO and BBPSO are not so good in the three damage cases under no noise conditions and under noise conditions. As for BBPSODJ, the performance of no noise conditions is very good, and there are some tiny identification errors, but the damage location and extent can be detected accurately. At the same time, however, GA has the poor capability in quantifying damage. Figure 6 demonstrates the superiority of BBPSODJ in compound condition than PSO, BBPSO, and GA.

5. Experiment Example

5.1. Vibration Test. To further assess the performance of BBPSODJ, a 3-story steel frame model, which is shown in Figure 7, is applied here [47]. The frame model was constructed using three steel plates of 850 mm × 500 mm × 25 mm and four rectangular columns with section area of 9.5 mm × 75 mm. The connections between plates and columns were rigid. Then, the four columns

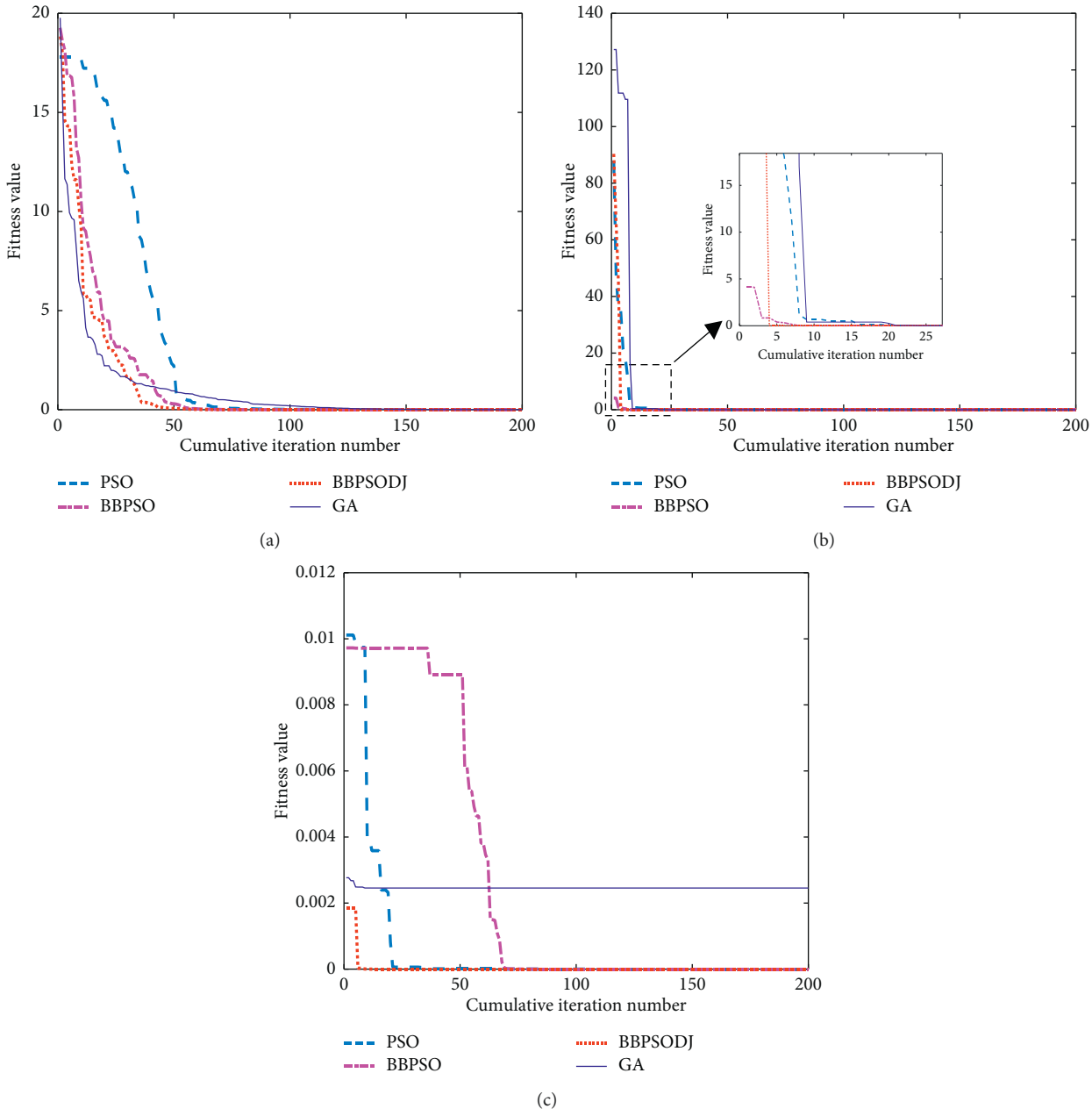

Figure 4: Iterative curves of test function: (a) Ackley; (b) Schwefel; (c) Schaffer.

were welded on a steel base plate of 20 mm thickness. The model was anchored into a shaking table by 8 bolts with high tensile strength. The height, length, and width of the frame model were 1450 mm × 850 mm × 500 mm. In addition, every floor was placed an additional mass block of 135 kg to simulate the actual floor weight; after that, the mass of each floor is 213 kg. More details of the test and model are shown in the paper [47]. The overall, plan, and simplified model of the steel frame model are shown in Figure 8.

5.2. Model Updating Using BBPSODJ. The finite element model of the steel frame structure is developed based on MATLAB. However, there are some errors between the experimental model and the finite element model, and the finite element model needs to be updated before the process of SDI.

The comparison of the experimental and analytical natural frequencies before and after updating is shown in Table 2. It is obvious that the errors between the finite element model and the experimental model are small, and the capability of model updating of BBPSODJ has been verified.

The finite element model of the steel frame structure after updating can be utilized as a benchmark structure for the subsequent damage identification. The structural damage was introduced by the cut of cross section of the column (Figure 9). Four damage cases were considered, which are listed in Table 3. For single damage case, case 1 and case 2,

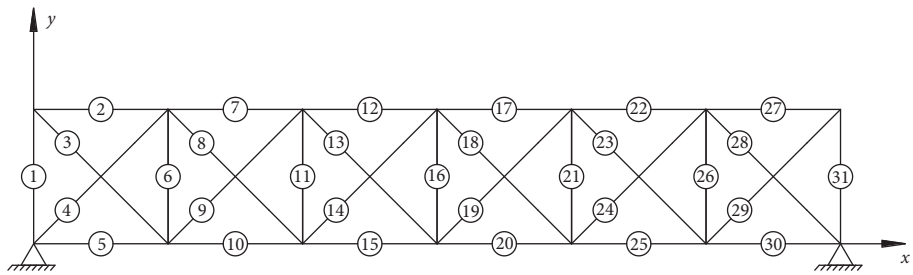

Figure 5: 31-bar truss structure.

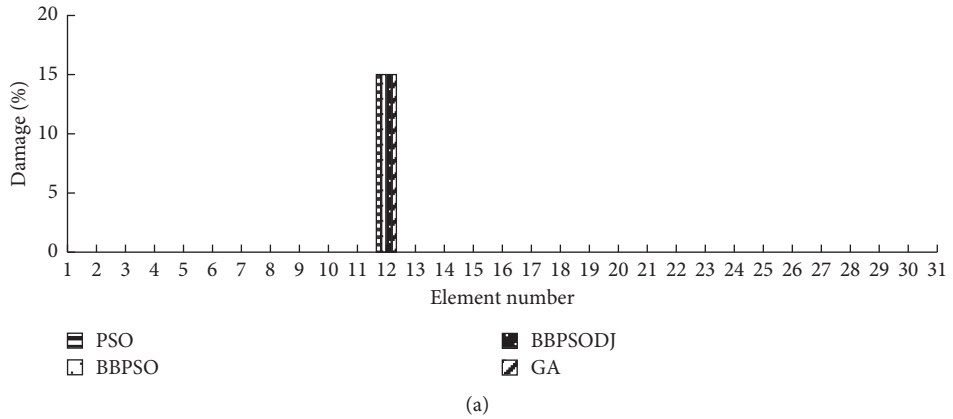

(a)

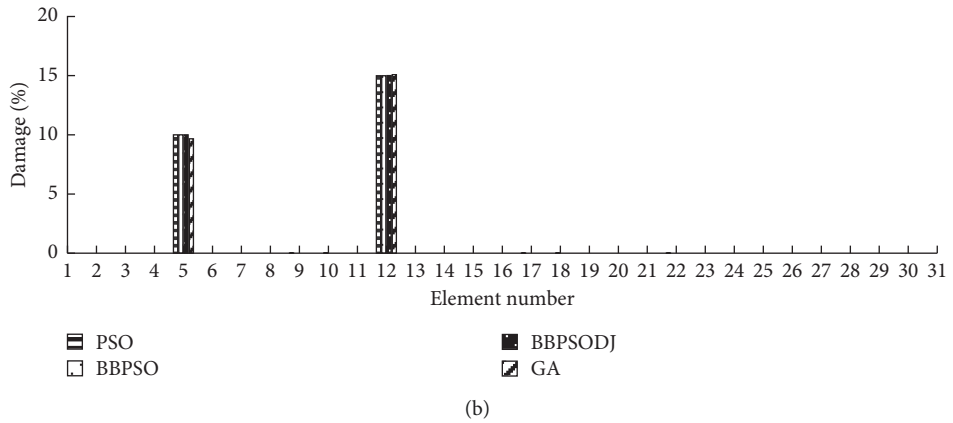

(b)

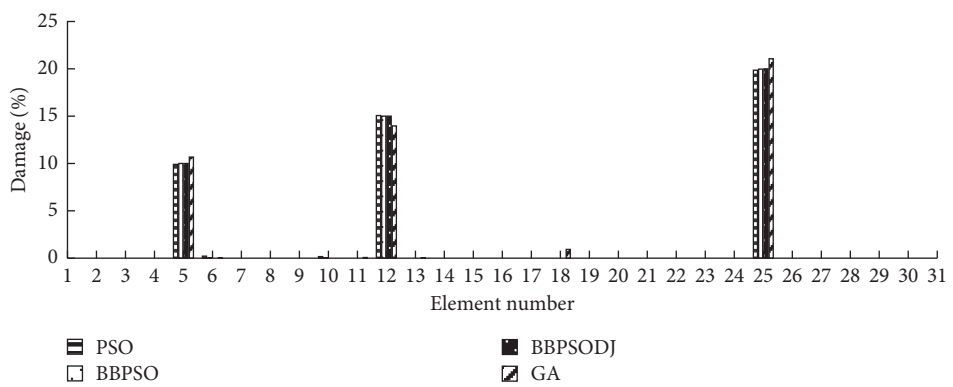

(c)

Figure 6: Continued.

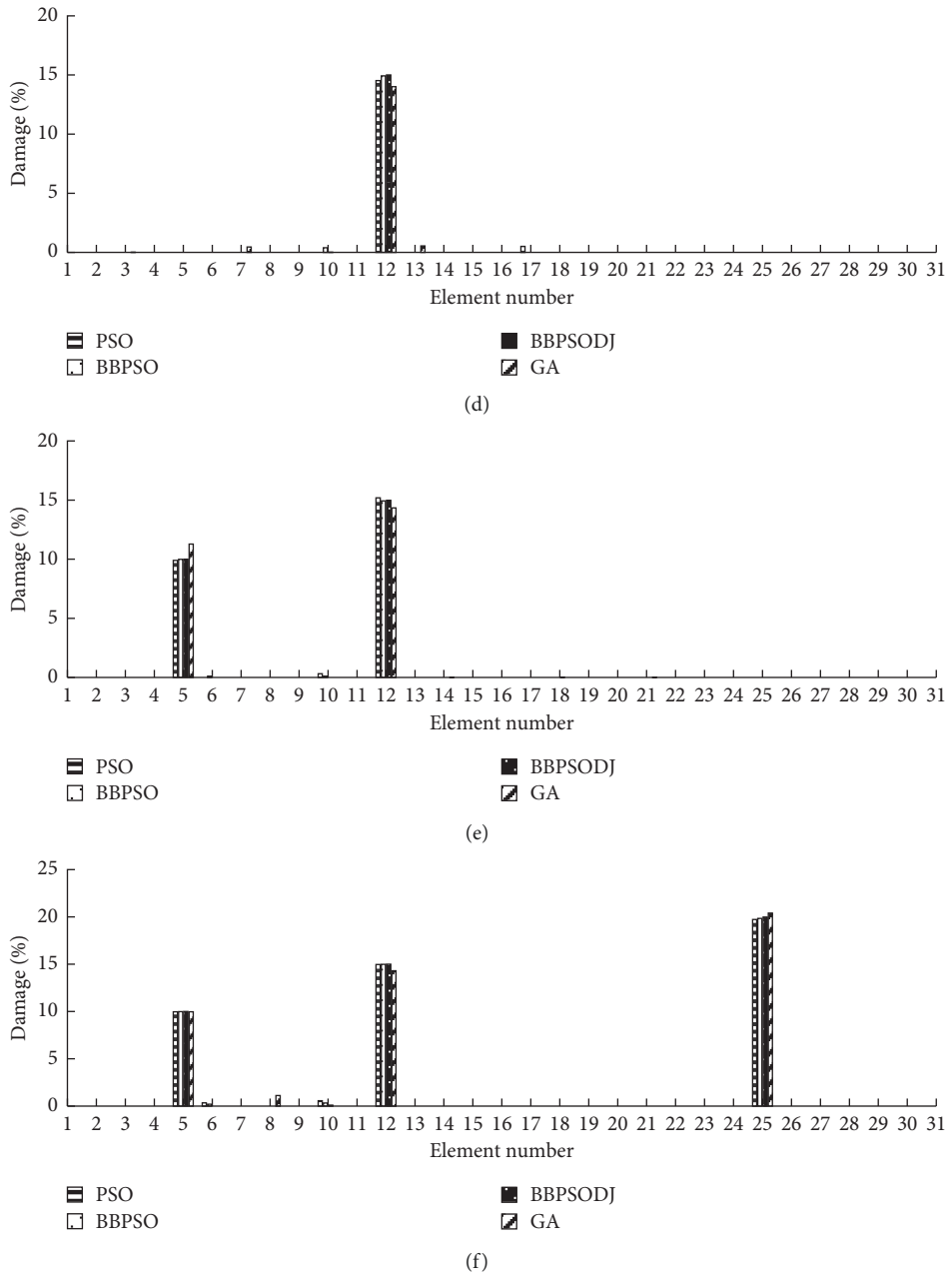

Figure 6: Damage identification results of 31-bar truss structure: (a) case 1; (b) case 2; (c) case 3; (d) case 4; (e) case 5; (f) case 6.

the cutting width of the columns on the first floor was 23.7 mm and 37.54 mm, respectively; and for multiple damage case, case 3 based on case 2, the cutting width in the second floor was 23.7 mm. For case 4, the cutting width on the first floor and the second floor was both 37.54 mm. The equivalent damage severity can be calculated as follows [48]:

$$\beta = \frac{1}{2\left(\gamma\alpha^4 - 4\gamma\alpha^3 + 6\gamma\alpha^2 - 4\gamma\alpha + \gamma - 1 + \alpha\right)}\left(\alpha\left(1 + 2\gamma\alpha^3 - 4\gamma\alpha^2 + 6\gamma\alpha - 4\gamma - \sqrt{1 - 8\gamma - 4\gamma\alpha^2 + 12\gamma\alpha + 16\gamma^2\alpha^4 - 48\gamma^2\alpha^3 + 64\gamma^2\alpha^2 - 48\gamma^2\alpha + 16\gamma^2}\right)\right), \tag{22}$$

where β is the ratio of inertia moment between the cutting width and the uncut width, α is the ratio of cutting width, and γ is the ratio of stiffness between the cut column and the intact column.

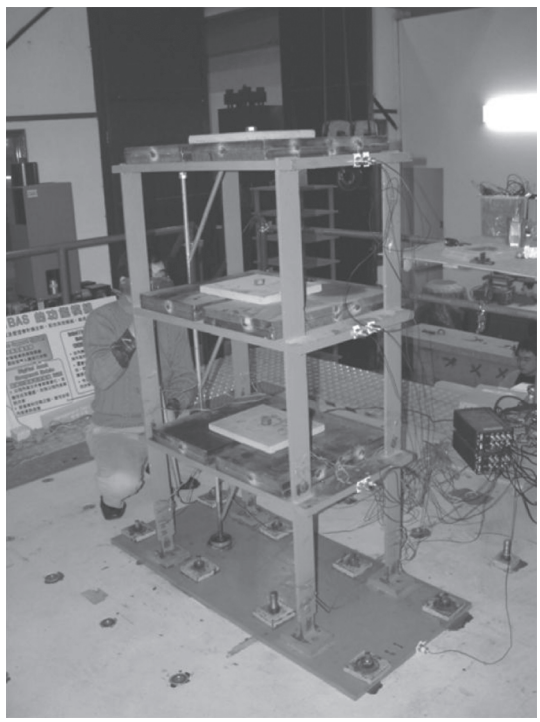

Figure 7: The 3-story steel frame.

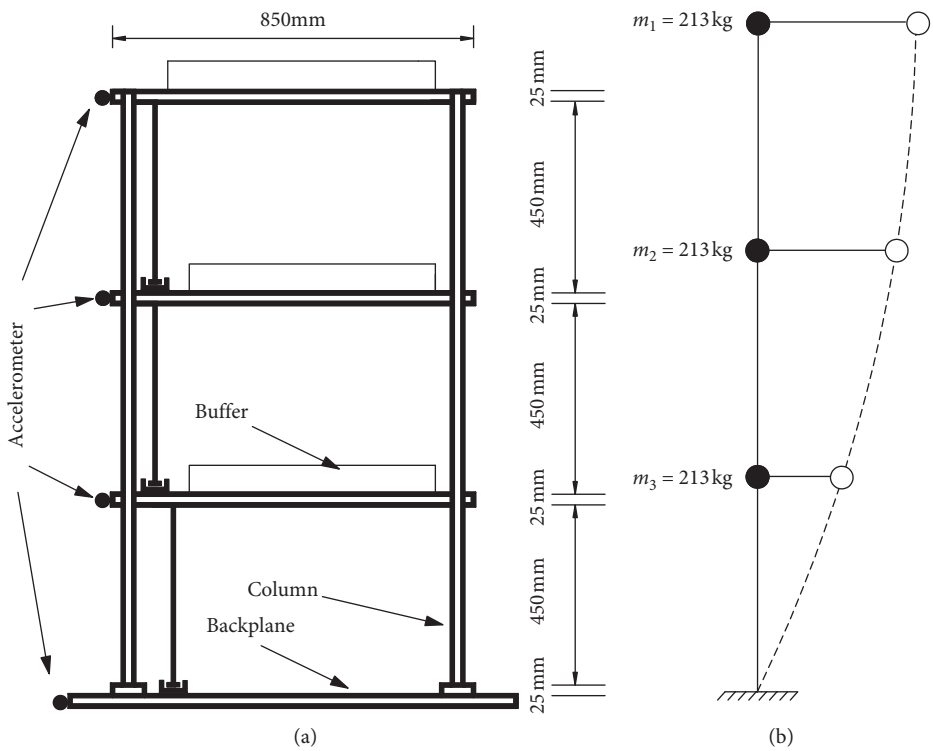

Figure 8: Continued.

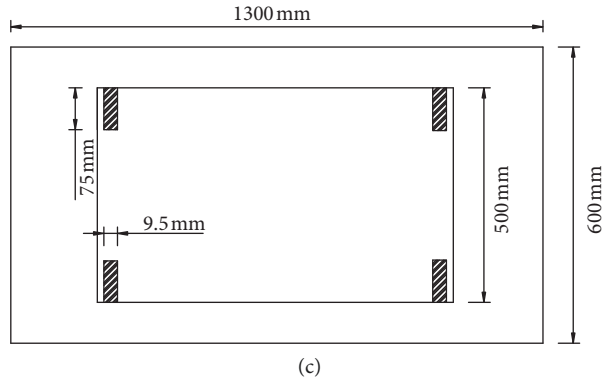

Figure 8: Steel frame model: (a) overall; (b) simplified model; (c) plan.

Table 2: Experimental and analytical natural frequencies for the undamaged frame structure.

		Before updating		After updating	
Mode	Experimental (Hz)	Analytical (Hz)	Error (%)	Analytical (Hz)	Error (%)
1	3.369	3.449391	0.285	3.36902	0.0005
2	9.704	9.681222	0.235	9.70401	0.0001
3	14.282	14.018233	1.847	14.2819	0.0007

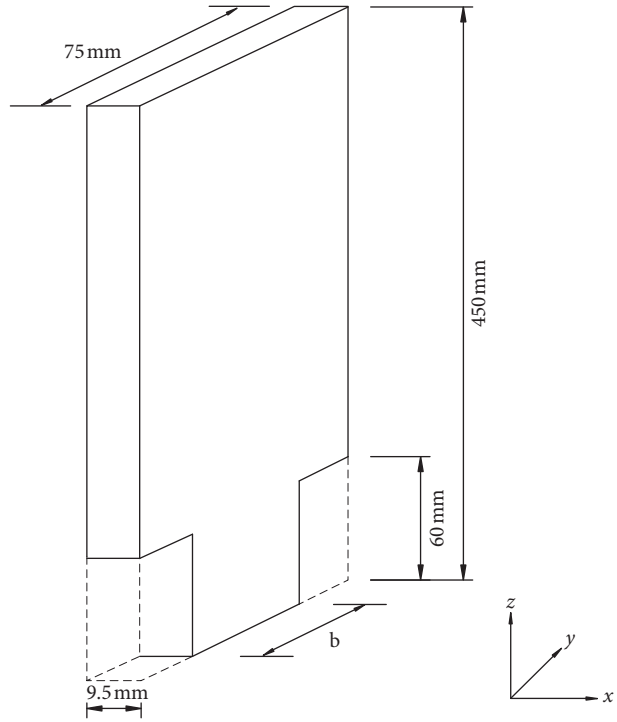

Figure 9: Column size.

For 4 damage cases, the experimental and analytical modal parameters are shown in Table 4, which are obtained by measurement in laboratory and model updating by BBPSODJ. Then, the BBPSODJ algorithm is performed to distinguish damage based on the objective function which is proposed in Section 2.3. The findings are collected as shown in Figure 10.

From Figure 10, it can be seen that the damage identification results have small errors, but the damage of the steel frame structure can be precisely located and accurately quantified. Compared to the true damage as shown in Table 3, the minor false identification can be omitted. It is evident that the BBPSODJ algorithm with l_1 regularization

Table 3: Damage cases of steel frame structure.

Story	Undamaged		Damage case 1		Damage case 2		Damage case 3		Damage case 4	
	Cutting width	Damage (%)	Cutting width	Damage (%)	Cutting width	Damage (%)	Cutting width	Damage (%)	Cutting width	Damage (%)
1st	0	0	23.7 mm	11.6	37.54 mm	21.1	37.54 mm	21.1	37.54 mm	21.1
2nd	0	0	0	0	0	0	23.7 mm	11.6	37.54 mm	21.1
3rd	0	0	0	0	0	0	0	0	0	0

Table 4: Experimental and analytical natural frequencies for 4 damage cases.

Mode	Damage case 1		Damage case 2		Damage case 3		Damage case 4	
	Experimental (Hz)	Analytical (Hz)	Experimental (Hz)	Analytical (Hz)	Experimental (Hz)	Analytical (Hz)	Experimental (Hz)	Analytical (Hz)
1	3.259	3.2483	3.113	3.1347	3.076	3.0793	3.003	3.0242
2	9.485	9.5142	9.302	9.3534	9.192	9.2438	9.082	9.1321
3	14.209	14.2049	14.136	14.1456	13.660	13.6995	13.330	13.3393

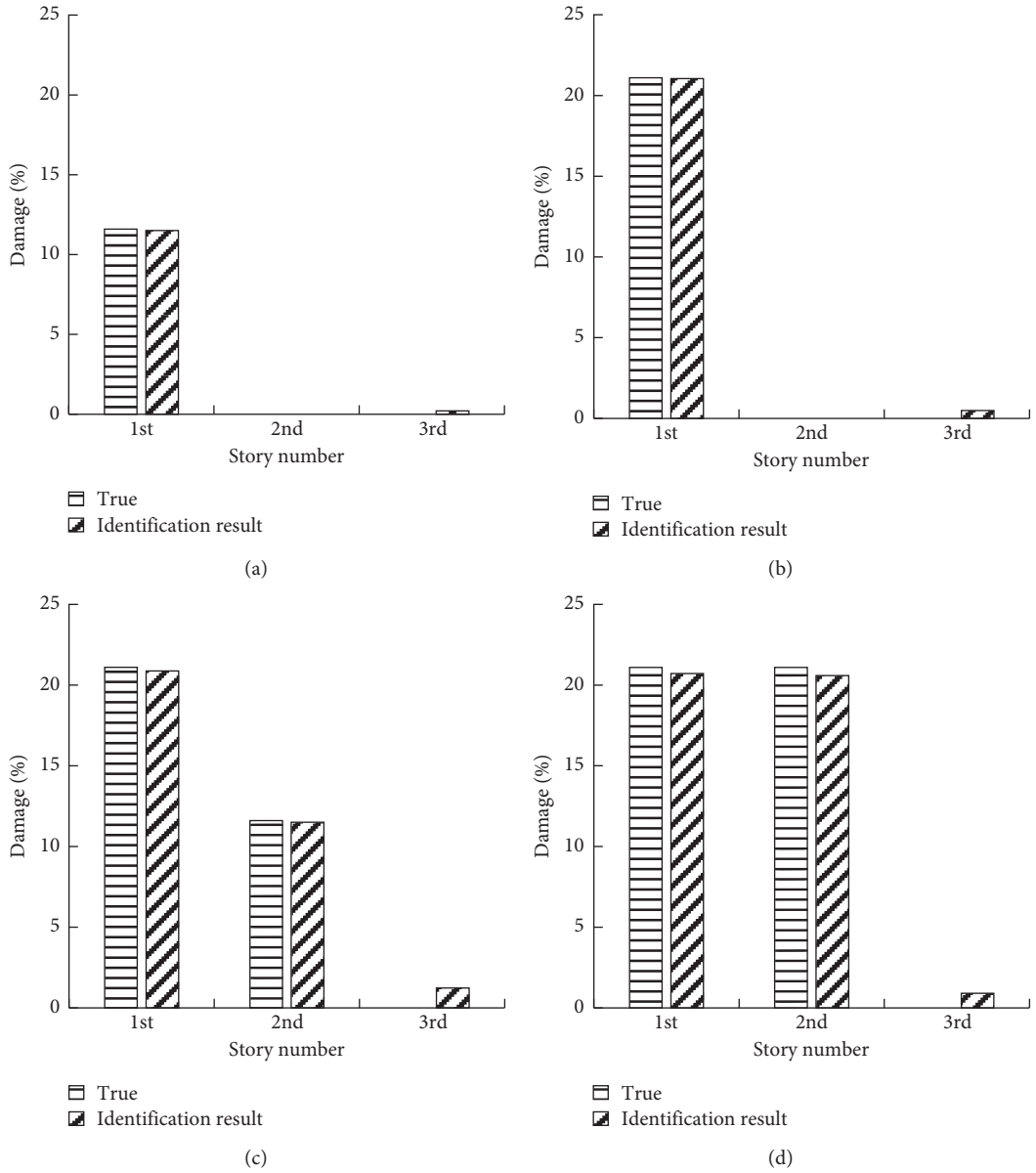

Figure 10: Damage identification results of steel frame structure: (a) damage case 1; (b) damage case 2; (c) damage case 3; (d) damage case 4.

approach can achieve greater effects on structural damage identification problems.

6. Conclusions

(1) The mathematical model of structural damage identification is established according to structural dynamics and finite element theories; meanwhile, a l_1 regularization objective function is constructed.

(2) An improved novel optimization algorithm, BBPSODJ, is first applied to solve the problem of SDI. Then, after the introduction of basic theory of BBPSO, a novel double jump strategy is incorporated into the basic BBPSO. Compared with basic BBPSO, traditional PSO, and GA, three optimization test functions are used to evaluate the search ability of the proposed algorithm, which indicate that BBPSODJ has faster convergence rate and better global search ability.

(3) A numerical example of 31-bar truss structure is utilized to evaluate the SDI performance of BBPSODJ, and BBPSODJ combined with l_1 regularization objective function shows significantly good performance in detecting multiple damage cases even under noisy environment. And in the laboratory, an experiment example of steel frame with 4 damage cases is considered to verify the feasibility of the proposed method to SDI problem. The test results show that although there are some small errors in the identification results, it can still detect the location and quantify the extent of damage well. The proposed BBPSODJ algorithm with high efficiency and good robustness has great potential in the field of SHM.

Data Availability

The data used to support the findings of this study are available from the corresponding author upon request.

Conflicts of Interest

The authors declare that there are no conflicts of interest regarding the publication of this paper.

References

[1] J. F. Gu, M. Gul, and X. G. Wu, "Damage detection under varying temperature using artificial neural networks," *Structural Control and Health Monitoring*, vol. 24, no. 11, Article ID e1998, 2017.

[2] X. Geng, S. Lu, M. Jiang et al., "Research on FBG-based CFRP structural damage identification using BP neural network," *Photonic Sensors*, vol. 8, no. 2, pp. 168–175, 2018.

[3] T. Yin and H.-P. Zhu, "Probabilistic damage detection of a steel truss bridge model by optimally designed Bayesian neural network," *Sensors*, vol. 18, no. 10, p. 3371, 2018.

[4] A. Anaissi, N. L. D. Khoa, and Y. Wang, "Automated parameter tuning in one-class support vector machine: an application for damage detection," *International Journal of Data Science and Analytics*, vol. 6, no. 4, pp. 311–325, 2018.

[5] R. Ghiasi, P. Torkzadeh, and M. Noori, "A machine-learning approach for structural damage detection using least square support vector machine based on a new combinational kernel function," *Structural Health Monitoring: An International Journal*, vol. 15, no. 3, pp. 302–316, 2016.

[6] Y. Yu, U. Dackermann, J. Li, and E. Niederleithinger, "Wavelet packet energy–based damage identification of wood utility poles using support vector machine multi-classifier and evidence theory," *Structural Health Monitoring*, vol. 18, no. 1, pp. 123–142, 2019.

[7] Y.-Z. Lin, Z.-H. Nie, and H.-W. Ma, "Structural damage detection with automatic feature-extraction through deep learning," *Computer-Aided Civil and Infrastructure Engineering*, vol. 32, no. 12, pp. 1025–1046, 2017.

[8] M. H. Rafiei and H. Adeli, "A novel machine learning-based algorithm to detect damage in high-rise building structures," *The Structural Design of Tall and Special Buildings*, vol. 26, no. 18, Article ID e1400, 2017.

[9] M. H. Rafiei and H. Adeli, "A novel unsupervised deep learning model for global and local health condition assessment of structures," *Engineering Structures*, vol. 156, pp. 598–607, 2018.

[10] Y. Gao and K. M. Mosalam, "Deep transfer learning for image-based structural damage recognition," *Computer-Aided Civil and Infrastructure Engineering*, vol. 33, no. 9, pp. 748–768, 2018.

[11] T. Guo, L. Wu, C. Wang, and Z. Xu, "Damage detection in a novel deep-learning framework: a robust method for feature extraction," *Structural Health Monitoring*, pp. 1–19, 2019.

[12] H. Liu and Y. Zhang, "Deep learning-based brace damage detection for concentrically braced frame structures under seismic loadings," *Advances in Structural Engineering*, vol. 22, no. 16, pp. 3473–3486, 2019.

[13] Y. Yu, C. Wang, X. Gu, and J. Li, "A novel deep learning-based method for damage identification of smart building structures," *Structural Health Monitoring*, vol. 18, no. 1, pp. 143–163, 2019.

[14] B. Huang and H. Chen, "A new approach for stochastic model updating using the hybrid perturbation -Garlekin method," *Mechanical Systems and Signal Processing*, vol. 129, pp. 1–19, 2019.

[15] H. F. Lam, J. H. Yang, and S. K. Au, "Markov chain Monte Carlo-based Bayesian method for structural model updating and damage detection," *Structural Control and Health Monitoring*, vol. 25, no. 4, Article ID e2140, 2018.

[16] M. Song, S. Yousefianmoghadam, M. E. Mohammadi, B. Moaveni, A. Stavridis, and R. L. Wood, "An application of finite element model updating for damage assessment of a two-story reinforced concrete building and comparison with lidar," *Structural Health Monitoring*, vol. 17, no. 5, pp. 1129–1150, 2018.

[17] M. S. Huang, M. Gul, and H. P. Zhu, "Vibration-based structural damage identification under varying temperature effects," *Journal of Aerospace Engineering*, vol. 31, no. 3, Article ID 04018014, 2018.

[18] M. S. Huang, Y. Z. Lei, and S. X. Cheng, "Damage identification of bridge structure considering temperature variations based on particle swarm optimization-cuckoo search algorithm," *Advances in Structural Engineering*, vol. 22, no. 15, pp. 3262–3276, 2019.

[19] Z. H. Ding, M. Huang, and Z. R. Lu, "Structural damage detection using artificial bee colony algorithm with hybrid

search strategy," *Swarm and Evolutionary Computation*, vol. 28, pp. 1–13, 2016.

[20] H. Gökdağ and A. R. Yildiz, "Structural damage detection using modal parameters and particle swarm optimization," *Materials Testing*, vol. 54, no. 6, pp. 416–420, 2012.

[21] C.-D. Pan, L. Yu, Z.-P. Chen, W.-F. Luo, and H.-L. Liu, "A hybrid self-adaptive Firefly-Nelder-Mead algorithm for structural damage detection," *Smart Structures and Systems*, vol. 17, no. 6, pp. 957–980, 2016.

[22] L. Yu and C. Li, "A global artificial fish swarm algorithm for structural damage detection," *Advances in Structural Engineering*, vol. 17, no. 3, pp. 331–346, 2014.

[23] Y. Hu, "Hybrid-fitness function evolutionary algorithm based on simplex crossover and PSO mutation for constrained optimization problems," *International Journal of Pattern Recognition and Artificial Intelligence*, vol. 23, no. 1, pp. 115–127, 2009.

[24] Y. He, A. Wang, H. Su, and M. Wang, "Particle swarm optimization using neighborhood-based mutation operator and intermediate disturbance strategy for outbound container storage location assignment problem," *Mathematical Problems in Engineering*, vol. 2019, Article ID 9132315, 13 pages, 2019.

[25] J. Kennedy, "Bare bones particle swarms," in *Proceedings of the 2003 IEEE Swarm Intelligence Symposium*, pp. 80–87, Indianapolis, IN, USA, April 2003.

[26] J. Guo and Y. Sato, "A pair-wise bare bones particle swarm optimization algorithm," in *Proceedings of the 2017 IEEE/ACIS 16th International Conference on Computer and Information Science*, pp. 353–358, Wuhan, China, 2017.

[27] J. Guo and Y. Sato, "A dynamic reconstruction bare bones particle swarm optimization algorithm," in *Proceedings of the 2018 IEEE Congress on Evolutionary Computation*, pp. 1–6, Rio de Janeiro, Brazil, July 2018.

[28] J. Guo and Y. Sato, "A fission-fusion hybrid bare bones particle swarm optimization algorithm for single-objective optimization problems," *Applied Intelligence*, vol. 49, no. 10, pp. 3641–3651, 2019.

[29] J. Guo and Y. Sato, "A bare bones particle swarm optimization algorithm with dynamic local search," in *Proceedings of the 2017 International Conference on Swarm Intelligence*, pp. 158–165, Fukuoka, Japan, August 2017.

[30] H. Liu, G. Ding, and B. Wang, "Bare-bones particle swarm optimization with disruption operator," *Applied Mathematics and Computation*, vol. 238, pp. 106–122, 2014.

[31] H. Liu, G. Xu, G. Ding, and D. Li, "Integrating opposition-based learning into the evolution equation of bare-bones particle swarm optimization," *Soft Computing*, vol. 19, no. 10, pp. 2813–2836, 2015.

[32] R. A. Krohling and E. Mendel, "Bare bones particle swarm optimization with Gaussian or Cauchy jumps," in *Proceedings of the 2009 IEEE Congress on Evolutionary Computation*, pp. 3285–3291, Trondheim, Norway, 2009.

[33] J. W. Lee, T. Choi, and H. Do, "Experimental results of heterogeneous cooperative Bare Bones Particle Swarm Optimization with Gaussian jump for large scale global optimization," in *Proceedings of the 2015 IEEE Congress on Evolutionary Computation*, pp. 1979–1985, Sendai, Japan, May 2015.

[34] C. Qiu, "Bare bones particle swarm optimization with adaptive chaotic jump for feature selection in classification," *International Journal of Computational Intelligence Systems*, vol. 11, no. 1, pp. 1–14, 2018.

[35] C. Zeng and Y. Shen, "A distribution-guided bare-bones particle swarm optimization," in *Proceedings of the 2016 12th International Conference on Natural Computation*, pp. 150–154, Fuzzy Systems and Knowledge Discovery, Changsha, China, 2016.

[36] M. M. Al-Rifaie and T. Blackwell, "Bare bones particle swarms with jumps," in *Proceedings of the Swarm Intelligence—8th International Conference*, pp. 49–60, Brussels, Belgium, September 2012.

[37] X.-Q. Zhou, Y. Xia, and S. Weng, "L_1 regularization approach to structural damage detection using frequency data," *Structural Health Monitoring: An International Journal*, vol. 14, no. 6, pp. 571–582, 2015.

[38] R. Hou, Y. Xia, and X. Q. Zhou, "Structural damage detection based on l_1 regularization using natural frequencies and mode shapes," *Structural Control and Health Monitoring*, vol. 25, no. 3, Article ID e2107, 2018.

[39] R. Hou, Y. Xia, Y. Bao, and X. Zhou, "Selection of regularization parameter for l_1-regularized damage detection," *Journal of Sound and Vibration*, vol. 423, pp. 141–160, 2018.

[40] C. D. Zhang and Y. L. Xu, "Comparative studies on damage identification with Tikhonov regularization and sparse regularization," *Structural Control and Health Monitoring*, vol. 23, no. 3, pp. 560–579, 2016.

[41] P. C. Hanse, "The *L*-curve and its use in the numerical treatment of inverse problems," *Advances in Computational Bioengineering*, vol. 5, p. 119, 2001.

[42] R. J. Allemang, "The modal assurance criterion–twenty years of use and abuse," *Sound and Vibration*, vol. 37, pp. 14–23, 2003.

[43] R. Eberhart and J. Kennedy, "Particle swarm optimization," in *Proceedings of the IEEE International Conference on Neural Networks*, pp. 1942–1948, Perth, Australia, December 1995.

[44] M. Clerc, "The swarm and the queen: towards a deterministic and adaptive particle swarm optimization," in *Proceedings of the 1999 Congress on Evolutionary Computation-CEC99*, pp. 1951–1957, Los Alamitos, CA, USA, July 1999.

[45] Y. Shi and R. Eberhart, "A modified particle swarm optimizer," in *Proceedings of the 1998 IEEE International Conference on Evolutionary Computation*, pp. 69–73, Anchorage, AK, USA, May 1998.

[46] A. Rasouli, S. S. Kourehli, G. Ghodrati Amiri, and A. Kheyroddin, "A two-stage method for structural damage prognosis in shear frames based on story displacement index and modal residual force," *Advances in Civil Engineering*, vol. 2015, Article ID 527537, 15 pages, 2015.

[47] H. P. Zhu and Y. L. Xu, "Damage detection of mono-coupled periodic structures based on sensitivity analysis of modal parameters," *Journal of Sound and Vibration*, vol. 285, no. 1-2, pp. 365–390, 2005.

[48] L. Li, *Numerical and experimental studies of damage detection for shearing buildings*, Ph.D. thesis, Huazhong University of Science and Technology, Wuhan, China, 2005.